Changes in chemical composition of carbides in 2·25Cr–1Mo power plant steel Part 1 Bainitic microstructure

R. C. Thomson and H. K. D. H. Bhadeshia

The microstructure of a power plant steel changes during elevated temperature service. These changes in effect provide a built in time–temperature recorder which can be used in remanent life assessments. Hence, extensive studies have been undertaken of cementite composition changes as a function of time and temperature in a 2·25Cr–1Mo steel with a fully bainitic microstructure. The results are interpreted theoretically using a model for the enrichment of carbides as a function of heat treatment and steel chemistry. The results confirm the validity of the model, although further work is needed to predict the onset of alloy carbide formation at the expense of cementite. *MST/1895*

 Manuscript received 23 April 1993; in final form 9 June 1993. *The authors are in the Department of Materials Science and Metallurgy, University of Cambridge/JRDC.*

Introduction

The steel 2·25Cr–1Mo is used widely for superheater tubing in power plant, and as a filler metal for joining 0·5Cr–0·5Mo–0·25V steam piping. There has been much effort in the power generation industry over recent years to determine the remaining creep life of components which have been in service for a significant fraction of their design lifetimes. The prediction of remanent life requires a knowledge of service stresses and temperatures. The stresses can in principle be calculated accurately using finite element methods. However, temperature data are subject to considerable scatter due to spatial variations around the component and irregular fluctuations with time as a result of changes in the mode of plant operation. It has been proposed that time and temperature dependent microstructural parameters, such as carbide composition, can be used to estimate the thermal history of a component at any time during service.[1,2]

The methodology of estimation must be based on physical principles in order to ensure a safe interpretation of carbide chemistry data. Hence, considerable effort has recently been devoted to the development of a model describing the chemical changes to be expected when power plant steels are aged at elevated temperatures.[3–5] The purpose of the present work is to provide further detailed verification of the model. There is also a need to investigate the changes in cementite enrichment behaviour during the onset of alloy carbide precipitation. Of particular use for the latter purpose is 2·25Cr–1Mo steel since alloy carbide precipitation at typical service temperatures occurs within a timescale of a few hundred hours.[6] Such times are long enough to fully characterise the independent enrichment of cementite, but sufficiently short to study the later influence of alloy carbide formation on the stability of cementite.

Experimental

MATERIALS

The 2·25Cr–1Mo* steel was supplied by National Power in the form of a cylindrical bar approximately 100 mm in diameter and 300 mm in length. Rectangular specimens of size 10 × 10 × 60 mm were machined from the bar for furnace heat treatment, and smaller cylindrical specimens 8 mm in diameter and 12 mm in length were also machined for use in a thermomechanical simulator. The chemical composition of the steel is given in Table 1.

* All compositions are in wt-% unless stated otherwise.

MICROSCOPY

Samples for optical microscopy were etched in 2% nitric acid in methanol. Carbon replica and thin foil specimens were examined in a Philips 400T transmission electron microscope operated at 120 kV. The carbon extraction replicas were prepared from the metallographic samples with a lighter etch, following Smith and Nutting.[7] Electrolytic etching in a solution of 5% hydrochloric acid in methanol at +1·5 V was used to remove the carbon film, which was then washed in industrial methylated spirits, floated off in distilled water, and collected on copper grids. Thin foils were prepared from 3 mm discs mechanically punched from thin slices cut from the large rectangular specimens. The discs were mechanically ground to 50 μm thickness and then twin jet electropolished at 50 V in a solution of 5% perchloric acid, 20% glycerol, and 75% methanol cooled to 0°C.

ENERGY DISPERSIVE X-RAY ANALYSIS

A Link series 860 energy dispersive X-ray (EDX) spectrometer was used to carry out detailed microanalyses on particles in the extraction replica specimens. At least 30 isolated particles in each specimen were analysed, depending on the observed composition variation, covering an area of several grid squares. X-ray spectra were recorded at a specimen tilt of 35° and lifetimes of at least 200 s were used, depending on the count rate from individual particles. The dead time was not allowed to exceed 25%. Link RTS2 FLS software was used to analyse the data. The chemical data are reported without absorption or fluorescence corrections because of the irregular size and shape of the particles studied. The chromium concentration is of greatest interest and such corrections are minor for chromium at a typical particle thickness of <1 nm. Chromium was used as the best indicator of composition change; the molybdenum data are likely to be flawed due to the neglect of the absorption corrections.

PARTICLE SIZE MEASUREMENTS

Particle size is expressed in terms of a mean linear intercept, determined manually by measuring a number of random intercepts across each particle on a photographic negative. This measure relates directly to the diffusion distance across the particle and can be used for any geometry.

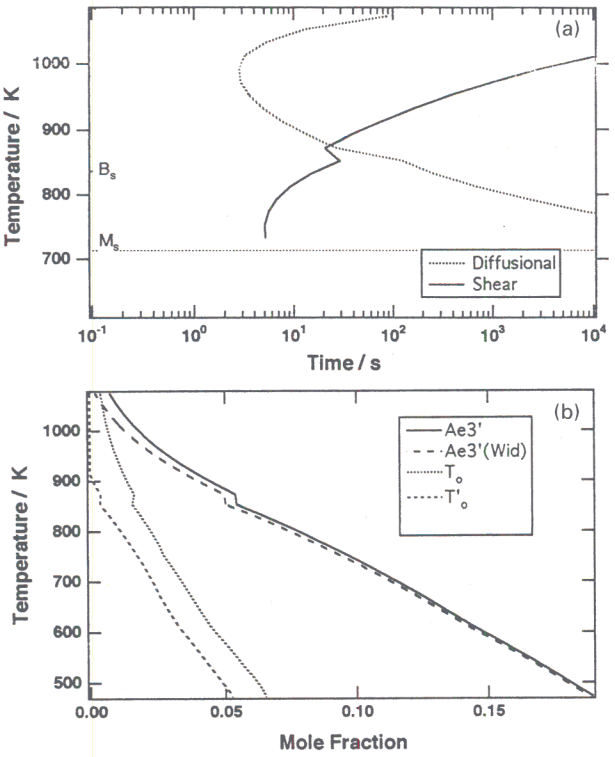

1 Calculated *a* time–temperature–transformation curve and *b* section of phase diagram for 2·25Cr–1Mo steel

HEAT TREATMENTS

The initial microstructure of power plant steels is formed during the continuous cooling of thick sections of material, resulting in a variety of mixtures of allotriomorphic ferrite, bainite, and martensite. The first part of this study focusses on a predominantly bainitic microstructure (containing some martensite); a mixed microstructure of allotriomorphic ferrite and bainite is discussed in Part 2 of this work.[8] The former microstructure is henceforth referred to as 'fully bainitic' for brevity, although it is recognised that it actually consists of a mixture of bainitic ferrite and martensite.

The time–temperature–transformation (TTT) and phase diagrams for the steel were calculated using a model developed by Bhadeshia.[9] The results are presented in Fig. 1. The phase diagram shows three distinct lines: the line T_0 is the locus of points where ferrite and austenite of identical composition have equal free energy and the line T'_0 is a modification of this which allows for the strain energy involved in the transformation (400 J mol^{-1}). The line Ae'_3 is the paraequilibrium phase boundary indicating equilibrium between ferrite and austenite when the ratio of iron to substitutional solute atoms is constant everywhere, i.e. when there is no substitutional alloying element partitioning during transformation. The start temperatures B_s and M_s for the bainite and martensite reactions respectively are marked on the TTT curve. The TTT curve was then used to determine a suitable heat treatment cycle.

The specimens were dip coated in a commerical application (containing a dispersion of clays and refractory solids in a solution of an organic resin in solvent) to limit any decarburisation which might occur during heat treatment. They were then austenitised at 1050°C for 15 min in a furnace before transfer into an adjacent fluidised bed at 480°C for 30 min and then water quenched. A scanning electron micrograph illustrating the predominantly bainitic microstructure with intervening islands of martensite is shown in Fig. 2. It is well known that the bainite reaction does not go to completion when cementite formation does not accompany the growth of bainite.[10] It is then possible to calculate the maximum expected volume fraction of bainite at 480°C using the equation

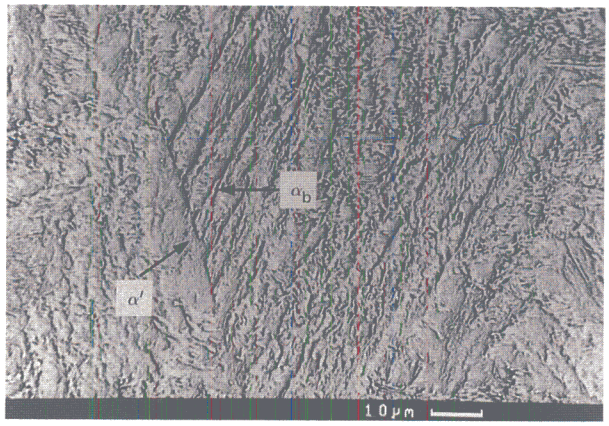

2 Starting bainitic microstructure (α_b and α' are bainitic and martensitic areas respectively) – austenitised 1050°C for 15 min, 480°C for 30 min, and then water quenched (SEM)

$$V_b \approx \frac{x_{T_0} - \bar{x}}{x_{T_0} - x_\alpha} \quad \ldots\ldots\ldots\ldots\ldots\ldots\ldots\ldots (1)$$

where x_{T_0} is the mole fraction of carbon remaining in austenite when the reaction stops, $\bar{x}$ is the average carbon concentration in the alloy, and x_α is the carbon concentration in bainitic ferrite (assumed to be 0). The phase diagram in Fig. 1*b* predicts a value for x_{T_0} of ~0·026 at 480°C and $\bar{x}$ is 0·0069, giving a volume fraction of ~0·7 at 480°C. This is in good qualitative agreement with Fig. 2. The initial microstructure was also characterised using transmission electron microscopy (TEM) on thin foil specimens. Figure 3 shows the bainitic α_b and martensitic α' area. A small amount of retained austenite was also noted in the martensitic regions.

Consistent with earlier observations,[10] cementite particles were not found immediately after isothermal transformation to this upper bainitic microstructure. The carbides in fact form later during high temperature tempering, from regions (martensitic or austenitic) in the microstructure which are relatively rich in carbon.

TEMPERING HEAT TREATMENTS

Before entering service 2·25Cr–1Mo steel is usually given a stress relief heat treatment at 700°C for several hours depending on the specimen size. This was avoided in the present work since the primary aim was to investigate changes in cementite composition in a detailed manner before the onset of alloy carbide formation.

Calculated enrichment of cementite

Power stations operate at temperatures close to 565°C, and therefore it was decided to temper the majority of the specimens at this temperature. Specimens were also

Table 1 Chemical composition of 2·25Cr–1Mo steel, wt-%

C	Si	Mn	P	S	Cr	Mo	Ni	Al	As	Co	Cu	Sn	V
0·15	0·29	0·49	0·01	0·025	2·20	0·96	0·14	<0·01	0·03	0·02	0·18	0·02	0·01

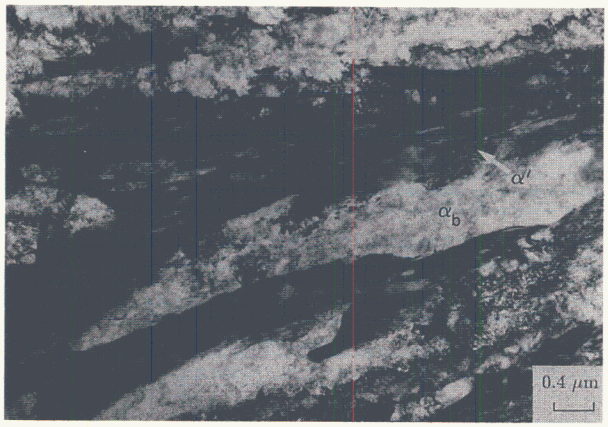

3 Mixture of bainite and martensite, martensite being heavily dislocated: there is also small amount of retained austenite – austenitised 1050°C for 15 min, 480°C for 30 min and then water quenched (TEM)

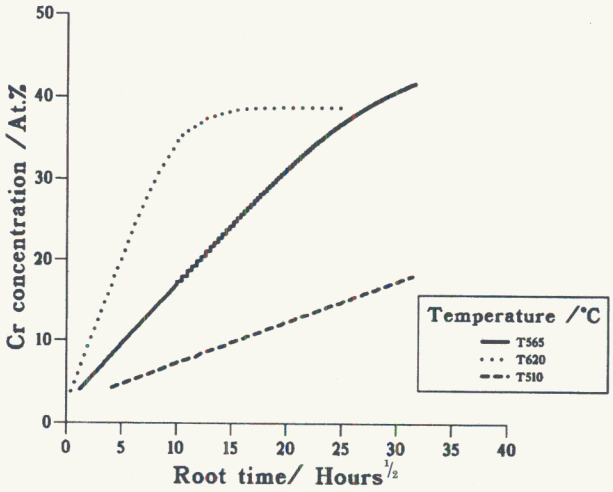

4 Calculated rate of cementite enrichment at 510, 565, and 620°C using finite difference model

tempered at 620 and 510°C in order to investigate the temperature dependence of enrichment rates. Appropriate tempering times at these temperatures were chosen using a computer model developed[3] to study the kinetics of composition changes in cementite composition during tempering. A finite difference method was used to provide numerical solutions to the equations governing the diffusion process, and also takes into account the overlap between the diffusion fields from adjacent particles (soft impingement). The model requires as input the equilibrium concentrations in the ferrite matrix and cementite and the diffusion coefficients of the substitutional element of interest, the temperature, and the particle size (in the manner described earlier as a mean linear intecept). The initial concentrations in the cementite and ferrite are simply the concentrations in the bulk alloy since it is assumed that there is no partitioning of the substitutional elements on transformation. The diffusion coefficients used are chemical interdiffusion coefficients,[11] with the diffusivity in cementite being assumed to be identical to that in ferrite.

The equilibrium chromium contents in cementite and ferrite as a function of temperature were determined using a computer package (Mtdata) in which the equilibria in multicomponent, multiphase systems are determined using critically assessed thermodynamic data.[12] The calculations could allow for all the major elements in the bulk alloy, and the phases M_3C, M_7C_3, M_6C, $M_{23}C_6$, M_2C, austenite, and ferrite. In order to calculate the equilibria between cementite and ferrite, cementite and ferrite were the only phases allowed to exist in the Mtdata calculations, and therefore the predicted rates of cementite enrichment do not take into consideration the effect of alloy carbide precipitation. This procedure will accurately predict the rate of cementite enrichment until the onset of alloy carbide precipitation, at which point the enrichment rate is observed to slow down. This is discussed in detail below in the subsections on coexistence of M_7C_3 with cementite and coexistence of M_2C with cementite. The calculated equilibrium chromium levels in cementite and ferrite at the temperatures of the tempering heat treatments are given in Table 2. The predicted volume fraction of cementite was 0·022; this was almost independent of temperature in the range of interest. Finite difference calculations were then carried out using these calculated equilibrium values to establish the interface concentrations. The calculations assumed an average particle size of 60 nm, determined via preliminary investigations using TEM. The results of the calculations are shown in Fig. 4. The tempering times at temperatures of 510, 565, and 620°C were established using the results of the calculations described above, and are presented in Table 3.

Table 2 Equilibrium chromium levels in cementite and ferrite calculated using Mtdata at temperatures of 510, 565, and 620°C

	Cementite		Ferrite	
Temperature, °C	at.-%	wt-%	at.-%	wt-%
510	51·51	61·99	0·95	0·88
565	45·22	53·99	1·13	1·05
620	38·91	46·11	1·32	1·23

Microstructural evolution during tempering at 565°C

A TEM image from a carbon extraction replica of the specimen tempered at 565°C for 10 min illustrating the early stages of carbide precipitation is shown in Fig. 5*a*. Cementite plates precipitated from carbon enriched austenite are visible at the bainitic ferrite lath boundaries. Figure 5*b* shows that further cementite precipitation has occurred after tempering for 64 h. Several carbides of each type were identified by selected area electron diffraction. Once an associated composition was found for each of these types, the composition alone could be used as a quick means of identifying the various types of carbide.[13]

After tempering for 128 h there is a noticeable difference in the precipitation behaviour within the bainitic and martensitic regions. This is illustrated in Figs. 6 and 7. Figure 6 shows that cementite precipitation occurs in the martensitic regions in the Widmanstätten pattern usually associated with the tempering of martensite. In Fig. 7 however, cementite precipitation in the bainitic regions can be seen mainly on the boundaries of the sheaves, whereas there is extensive precipitation of needle shaped M_2C within the sheaves coexisting with only a few cementite particles. The fine M_2C needles also precipitate in a regular

Table 3 Tempering heat treatment temperatures and times for the bainitic specimens

Temperature, °C	Time, h
510	1, 128, 256
565	$\frac{1}{6}$, 1, 4, 7, 32, 64, 128, 178, 239, 512, 1048, 2072
620	1, 10, 25

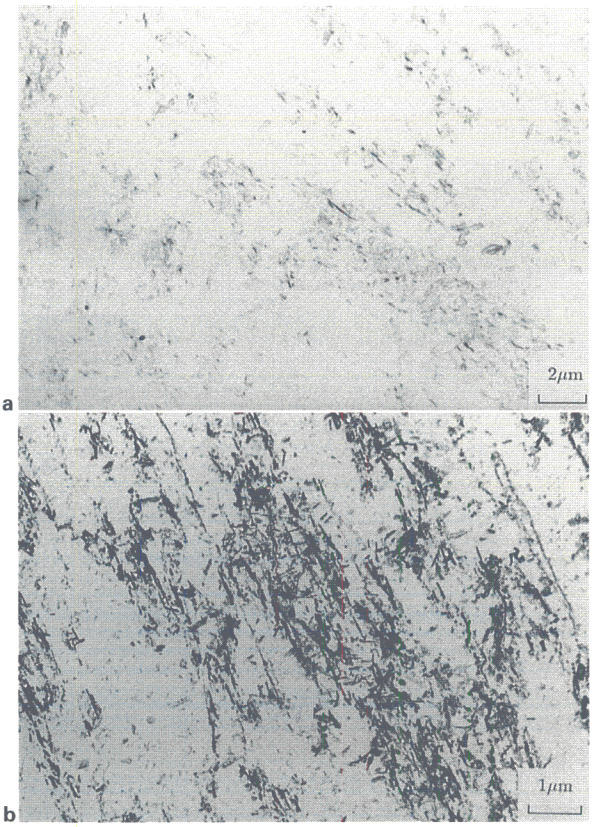

5 Carbon extraction replicas from fully bainitic specimens tempered for *a* 10 min and *b* 64 h at 565°C – *a* shows that cementite has begun to precipitate, in particular in between and parallel to plates of upper bainite

Widmanstätten array. The difference between the two regions is enhanced after prolonged tempering; Fig. 8*a* shows dense, Bagaryatski[14] oriented (Fig. 8*b*) cementite precipitates in the prior martensite regions but M_2C precipitation within the bainite in a specimen tempered for 178 h. Larger M_7C_3 particles can also be seen on the bainite lath boundaries.

Significant differences were found in the chemical composition of the cementite particles in the martensitic and bainitic regions. The typical composition of the cementite in martensite (not allowing for the carbon concentration) was found to be

25Cr–5Mn–7Mo–63Fe

whereas that in the bainite (adjacent to the M_2C) was relatively depleted in substitutional solutes

16Cr–6Mn–0·5Mo–77·5Fe

The M_2C in the bainitic regions was found to contain a considerable amount of dissolved chromium, a typical composition being

25Cr–0·5Mn–70·5Mo–4Fe

After 238·5 h tempering the microstructure consists predominantly of M_7C_3 and M_2C in all regions. The cementite in the bainitic regions has been replaced completely by M_2C with some larger M_7C_3 particles on the boundaries between sheaves. Some cementite with the higher chromium remains in the martensite, although there is also precipitation of M_7C_3 on the edges of these regions. The specimens tempered for 512 and 1048 h showed further precipitation of M_7C_3 at the expense of the cementite in the martensitic regions. All the cementite had dissolved in the specimen tempered for 1048 h (Fig. 9*a*). There was a slight enrichment

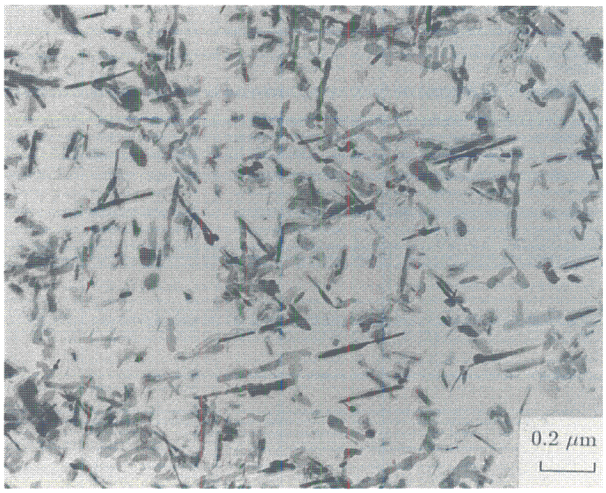

6 Cementite precipitation in martensitic regions of fully bainitic specimen tempered for 128 h at 565°C in Widmanstätten array

and growth of the M_7C_3 with respect to the chromium concentration with increasing tempering time. The carbide M_6C began to precipitate at the expense of some of the M_2C needles after 2072 h (Fig. 9*b*).

To summarise, carbide precipitation appears sensitive to location within the microstructure. Within the bainitic plates M_2C rapidly dominates whereas mixtures of M_2C, M_7C_3, and M_3C are found at the bainite plate boundaries and predominantly M_3C in the martensitic regions. This is probably because far less carbon is available within the upper bainitic plates, whereas more carbon is available at the plate boundaries and in the martensitic regions, where the cementite can survive for longer periods or indeed become an equilibrium phase alongside the alloy carbides.[15]

Carbide composition changes

The composition of isolated cementite particles was measured using EDX. A photograph was taken of each individual particle analysed in order to correlate the particle size with composition. Care was taken to ensure that unbiased distributions of particle sizes were studied. The

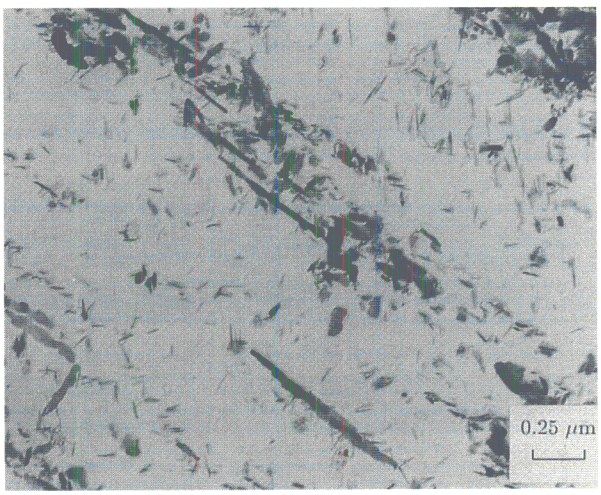

7 Carbon extraction replicas from specimen tempered at 565°C for 128 h showing cementite precipitation on boundaries of bainitic regions which contain extensive precipitation of M_2C needles in Widmanstätten array

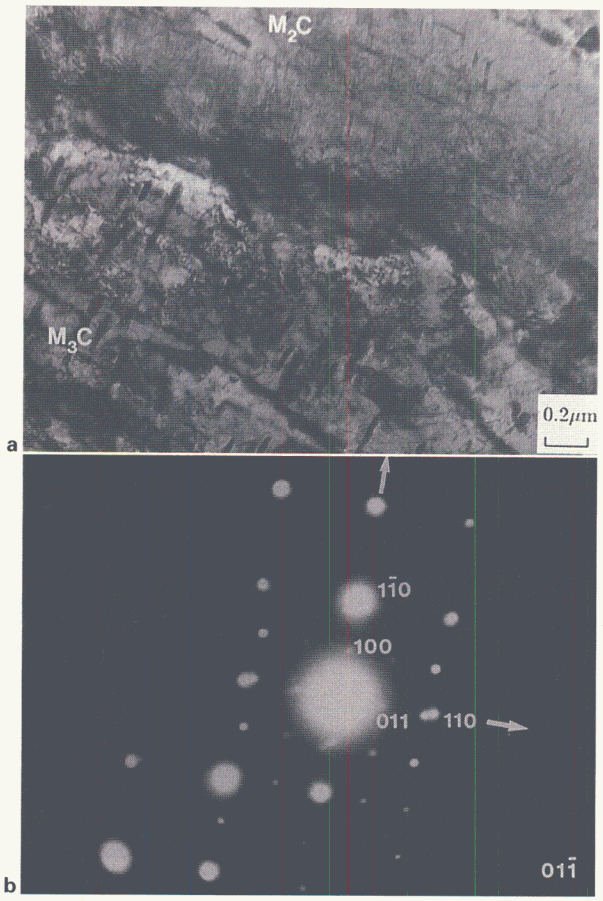

8 ***a*** **Thin foil from specimen tempered for 178 h at 565°C illustrating differences between different regions of microstructure (dense cementite precipitation in martensitic region and much finer M_2C precipitation in bainitic region and** ***b*** **selected area electron diffraction pattern from martensitic region exhibiting well known Bagaryatski[13] orientation relationship**

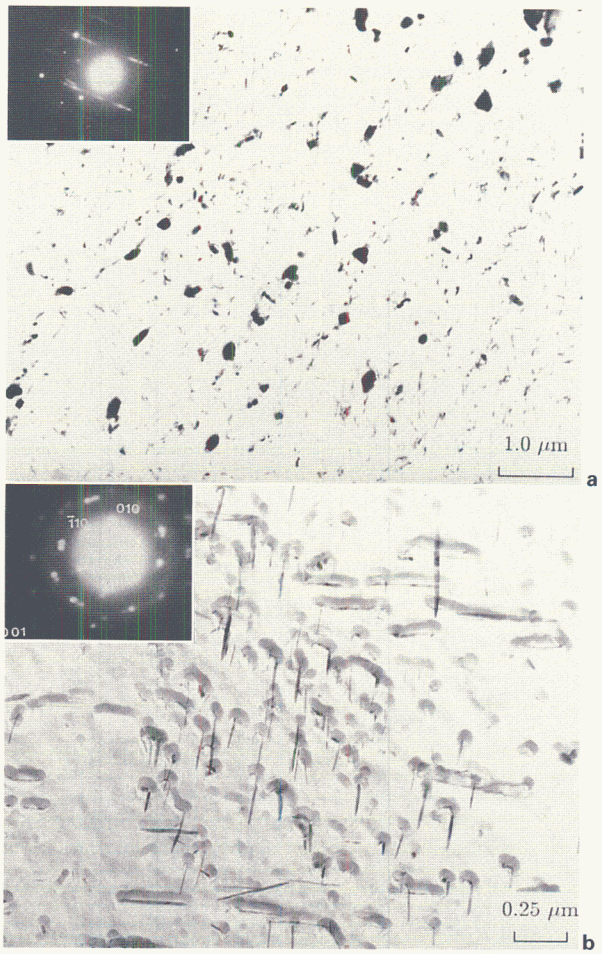

a microstructure consists predominantly of large M_7C_3 and fine M_2C particles – inset is selected area electron diffraction from M_7C_3 showing characteristic streaks due to presence of stacking faults within lattice; *b* aligned M_2C particles with small, squarer M_6C carbides in between – inset is selected area electron diffraction pattern from cluster of M_2C carbides

9 Carbon extraction replicas from specimen tempered for ***a*** **1048 and** ***b*** **2072 h at 565°C**

data are presented in Fig. 10 where the chromium concentration is plotted as a function of the reciprocal particle size for the specimens tempered up to 178 h at 565°C. The correlation coefficient about the regression line in each plot, the average particle size, and the average chromium concentration are given in Table 4.

Smaller particles are clearly richer in chromium, in spite of the scatter about the regression line. The correlation coefficient initially increased steadily with tempering time and then decreased. Theory predicts that the smaller particles should enrich at a faster rate than the larger particles so that the size dependence of concentration must become more pronounced with aging time. However, with prolonged tempering other effects remove the size dependence. These include the precipitation of alloy carbides and saturation of the carbides as they approach equilibrium. The very poor correlation coefficient in the measured chromium concentration for the 128 h specimen corresponds to the precipitation of the chromium rich M_7C_3.

It has already been noted that two separate populations of cementite were observed in the bainitic and martensitic regions of the microstructure. Figure 10*h* clearly shows the dichotomy of the cementite compositions; the upper points (triangles) are from martensitic regions of the microstructure free from alloy carbide precipitation whereas the lower points (circles) are from cementite particles in bainitic regions with extensive alloy carbide precipitation. The average chromium levels in the martensitic and bainitic regions are included in Table 4.

ENRICHMENT OF M_7C_3

The average composition (measured from at least 10 particles per specimen and not taking into account carbon content) of the M_7C_3 is given in Table 5. There was a gradual increase in the chromium concentration with tempering time, from 58·0 to 65·5 wt-%. The manganese correspondingly decreased with tempering time. The molybdenum data were scattered, probably due to the inherent difficulty in accounting for absorption errors. The alloy content also depends on the particles surrounding the M_7C_3 carbides. A similar effect to that already described for cementite particles in the vicinity of M_2C particles was observed; a few M_7C_3 carbides within clusters of M_2C needles contained very little molybdenum. No significant dependence of the composition on the particle size was observed for the M_7C_3.

Thermodynamic calculations were performed using Mtdata to investigate the equilibrium chromium levels of both M_7C_3–α and $M_{23}C_6$–α equilibria separately with ferrite. It was not possible to investigate the three phase equilibria, M_7C_3–M_2C–α and $M_{23}C_6$–M_2C–α. At equilibrium the predicted stable carbides in the temperature range 500–650°C are M_6C and $M_{23}C_6$, hence Mtdata will always predict that the M_2C has transformed to M_6C when carbides other than cementite are allowed to exist in the calculations. The calculations therefore provide an idea

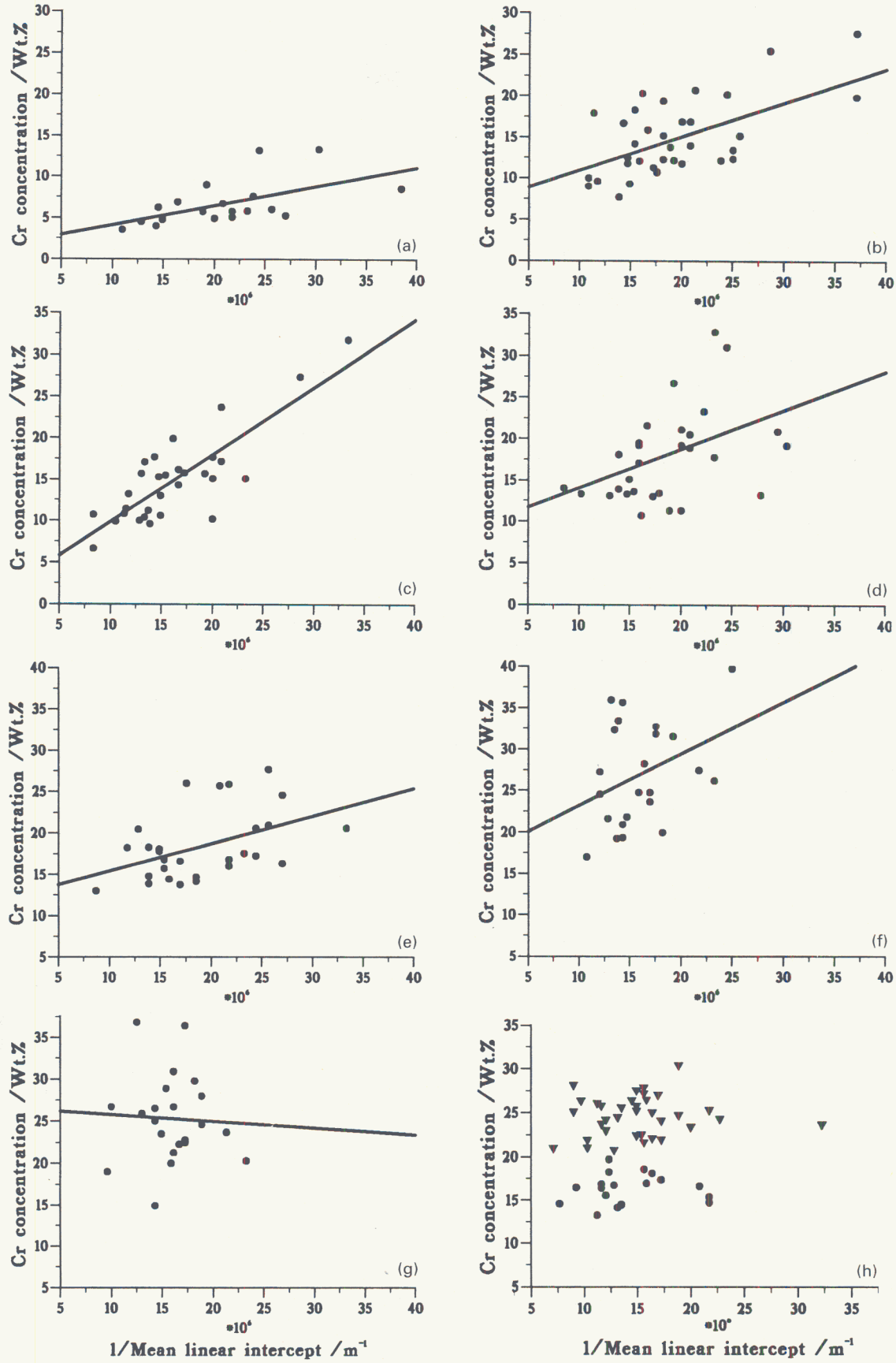

a 10 min; *b* 1 h; *c* 4 h; *d* 7 h; *e* 32 h; *f* 64 h; *g* 128 h; *h* 178 h (triangles are from martensitic regions of microstructure free from alloy carbide precipitation, and circles are from cementite particles in bainitic regions with extensive alloy carbide precipitation)

10 Chromium concentration in cementite plotted as function of reciprocal particle size for various tempering times at 565°C for fully bainitic microstructures of 2·25Cr–1Mo steel

Table 4 Summary of experimental measurements of chromium concentration and particle size for specimens tempered up to 178 h at temperature of 565°C

Tempering time, h	Correlation coefficient	Average chromium concentration, wt-%	Average particle size, nm
$\frac{1}{6}$	0·57	6·7	52
1	0·65	15·0	56
4	0·82	15·0	68
7	0·43	17·9	58
32	0·27	18·0	56
64	0·36	26·9	65
128	−0·05	25·3	65
178 (martensitic)	...	24·6	72
178 (bainitic)	...	16·3	75

of the chromium level only in each carbide because much of the molybdenum would, in practice, be tied up in M_2C in the real situation. The predicted equilibrium level of ~59%Cr in M_7C_3 at 565°C (Table 6) is in reasonable agreement with the EDX measurements (Table 5). The slight underestimation is because the calculations do not allow for the M_2C precipitation.

ENRICHMENT OF M_2C

It has been observed[16] that M_2C and M_6C become richer in molybdenum as a function of tempering time in a 2·25Cr–1Mo steel for tempering heat treatments carried out at 700°C. In the present study, the M_2C needles formed at 565°C were very fine and therefore attempts at measuring their compositions by EDX are subject to considerable error, especially with respect to the concentration of molybdenum. After 1048 h tempering, M_6C was found to precipitate and contained ~60%Mo which is in good agreement with the equilibrium composition calculated using Mtdata at 565°C. This is consistent with the lack of further enrichment on prolonged tempering. At the high temperatures used in the previous study,[16] the molybdenum based alloy carbides will precipitate quickly and therefore may not quite be at their equilibrium composition, whereas at lower temperatures they do not precipitate until much later tempering times. In this case the carbides were found to precipitate very close to their equilibrium compositions.

CARBIDE STABILITY

In order to establish the stable carbide at high tempering temperatures, a fully bainitic specimen was tempered at 750°C for 48 h to accelerate the precipitation of $M_{23}C_6$. The microstructure after this heat treatment (Fig. 11) consisted of two different carbide dispersions. The larger carbides were identified as $M_{23}C_6$ by both EDX and selected area electron diffraction (*see* inset), and the smaller

Table 5 Composition of M_7C_3 with tempering time at 565°C measured using energy dispersive X-ray analysis

	Concentration, wt-%			
Time, h	Cr	Mn	Mo	Fe
128	58	8	11	23
178	59	6	9	26
238·5	61	4·5	9	25·5
512	62	6·5	3	28·5
1048	63·5	5	7	24·5
2072	65·5	5	5	24·5

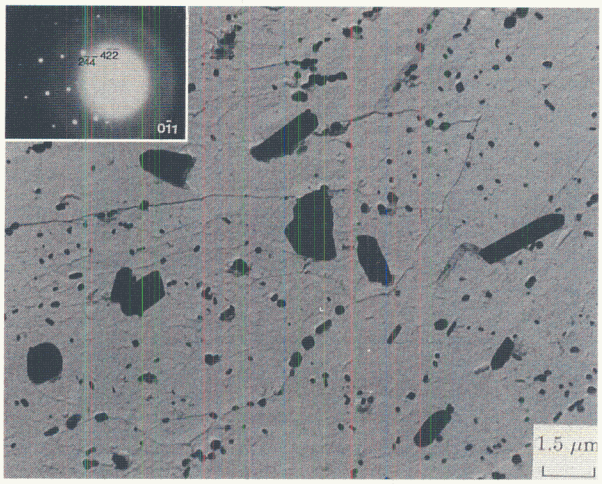

11 Carbon extraction replica from fully bainitic specimen tempered for 48 h at 750°C showing large particles of $M_{23}C_6$ and smaller M_7C_3 particles: inset is selected area electron diffraction pattern from $M_{23}C_6$ carbide

carbides as M_7C_3. The average composition of the $M_{23}C_6$ was

31Cr–2Mn–9Mo–58Fe

and that of the M_7C_3 was

51Cr–2·5Mn–7Mo–39·5Fe

These chromium levels are in very good agreement with those predicted using Mtdata (*see* Table 6) for tempering at 750°C. The amount of chromium each carbide can support increases as the tempering temperature decreases. The predicted chromium level in $M_{23}C_6$ at the lower temperature of 565°C is 48%. For tempering times up to 3000 h at 565°C $M_{23}C_6$ was not observed in the bainitic microstructure.

MICROSTRUCTURE DURING TEMPERING AT 510°C

As expected, the microstructural changes in specimens tempered at 510°C were considerably slower than at 565°C. Tempering for up to 256 h allowed cementite to precipitate and enrich as in the specimens tempered at 565°C. After 256 h M_2C precipitation was not found, compared with M_2C being found after 32 h in the specimens tempered at 565°C.

CHROMIUM CONTENT OF CEMENTITE AT 510°C

The plots of chromium concentration against the reciprocal of particle size are shown in Fig. 12 for the specimens

Table 6 Calculated equilibrium chromium levels in M_7C_3 and $M_{23}C_6$ as function of temperature using Mtdata scaled to remove stoichiometric carbon concentration to enable direct comparison with measurements obtained via energy dispersive X-ray analysis

	Cr level, wt-%	
Temperature, °C	M_7C_3	$M_{23}C_6$
750	52·2	30·4
700	54·5	34·5
650	56·5	39·2
600	58·0	44·4
565	58·7	48·2
550	58·8	49·8

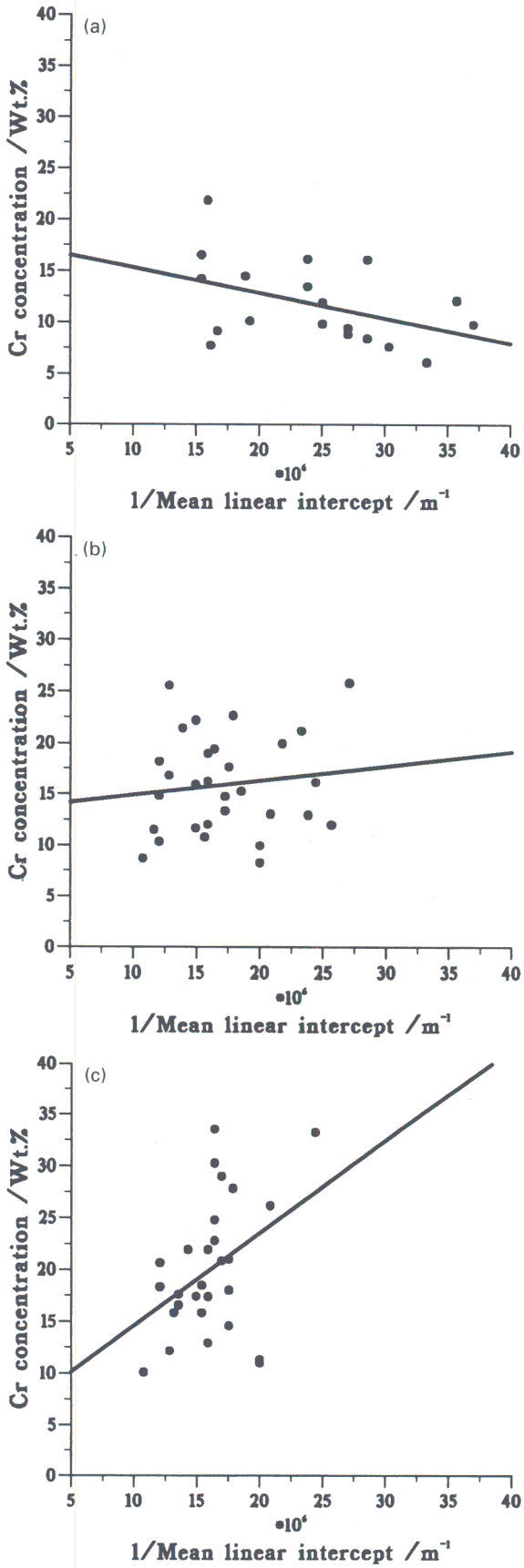

a 1 h; *b* 128 h; *c* 256 h

12 Chromium concentration in cementite plotted as function of reciprocal particle size for specimens tempered for various times at 510°C for fully bainitic microstructures of 2·25Cr–1Mo steel

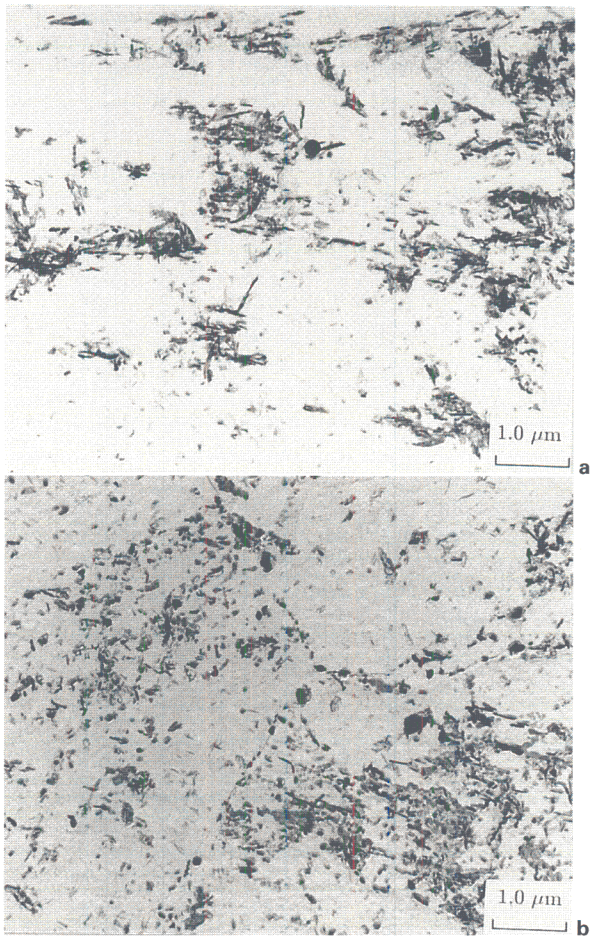

a relatively rapid cementite precipitation; *b* dense precipitation of M_7C_3

13 Carbon extraction replica taken from bainitic specimen tempered at 620°C for *a* 1 h and *b* 25 h

tempered at 510°C. There is considerable scatter in the compositions measured after tempering for 1 h but the slope of the regression line increases after tempering for 128 and 256 h as the effect of the smaller particles enriching more quickly than the larger particles becomes more prominent. The explanation for the apparent negative slope in Fig. 12*a* is that in the early stages of tempering when precipitation occurs, those particles which nucleate first (i.e. the larger particles in the size distribution) will in effect be tempered to a greater degree than those which nucleate later. Hence, the larger particles should at first be expected to be enriched to a greater degree. This effect should be most pronounced at short times and low temperatures since the enrichment process which follows precipitation soon overcomes the initial effects. The results of these analyses are summarised in Table 7.

Table 7 Summary of experimental measurements of chromium concentration in cementite and particle size for specimens tempered up to 256 h at 510°C

Tempering time, h	Correlation coefficient	Average chromium concentration, wt-%	Average particle size, nm
1	−0·43	11·8	45
128	0·13	15·9	62
256	0·40	20·1	64

MICROSTRUCTURE DURING TEMPERING AT 620°C

Microstructural changes at 620°C were rapid compared to those at 565°C. This is illustrated in Fig. 13*a* which shows extensive cementite precipitation after tempering for only 1 h taken from a carbon extraction replica. After 10 h tempering there is extensive precipitation of M_7C_3 together with fine M_2C needles. After 25 h the precipitation of M_7C_3 is widespread, as shown in Fig. 13*b*. M_7C_3 did not appear until after tempering for 128 h at 565°C. As at 565°C, there were two different types of cementite, one richer in chromium and molybdenum, and one containing less chromium and virtually no molybdenum, in the specimens tempered for only 25 h at 620°C. The typical cementite composition in the bainitic regions was

15Cr–3Mn–0Mo–82Fe

whereas the cementite particles in the martensitic regions have an average composition

23Cr–4·5Mn–5Mo–67·5Fe

CHROMIUM CONTENT OF CEMENTITE AT 620°C

Plots of chromium concentration against the reciprocal of particle size are presented in Fig. 14 for the specimens tempered at 620°C for 1, 10, and 25 h respectively. These results exhibit considerably more scatter than do those at 510 and 565°C. The explanation of this is that microstructural changes are accelerated at the higher temperature with alloy carbide precipitation being present to some extent in all the specimens. The results are summarised in Table 8. The cementite started to dissolve (corresponding to a drop in the experimentally measured cementite concentrations) after only 25 h at 565°C. Figure 14*c* shows the differences in cementite compositions between the martensitic regions of the microstructure free from alloy carbide precipitation (triangles) whereas the lower points (circles) are from cementite particles in bainitic regions with extensive alloy carbide precipitation.

COEXISTENCE OF M_7C_3 WITH CEMENTITE

It has been noted that M_7C_3 precipitated while cementite was still present in the microstructure, and then the two coexisted for some time. The cementite in the immediate vicinity of M_7C_3 particles was found to have a lower chromium content than the average measured for an isolated cementite particle. It was thought that in the same manner that precipitation of M_2C appears to draw molybdenum from the cementite, precipitation of the chromium rich M_7C_3 drew chromium away from any cementite particles nearby. For example, a particular cementite particle adjacent to an M_7C_3 carbide, had a composition

19Cr–4Mn–1Mo–76Fe

whereas an isolated cementite particle of comparable size had a composition

24Cr–4Mn–6Mo–66Fe

Table 8 Summary of experimental measurements of chromium concentration and particle size for specimens tempered up to 25 h at 620°C

Tempering time, h	Correlation coefficient	Average chromium concentration, wt-%	Average particle size, nm
1	0·35	17·6	73
10	0·13	25·5	81
25 (martensitic)	0·14	23·2	79
25 (bainitic)	...	15·2	87

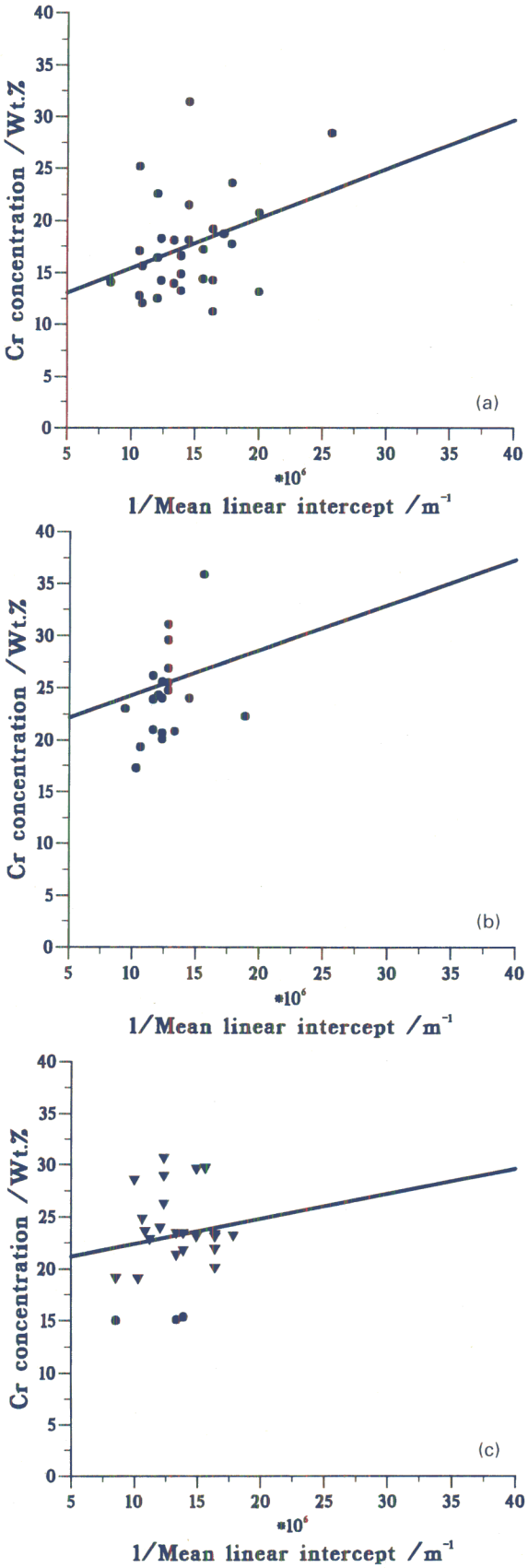

a 1 h; *b* 10 h; *c* 25 h (triangles are from martensitic regions of microstructure free from alloy carbide precipitation, and circles are from cementite particles in bainitic regions with extensive alloy carbide precipitation)

14 Chromium concentration in cementite plotted as function of reciprocal particle size for specimens tempered for various times at 620°C for fully bainitic microstructures of 2·25Cr–1Mo steel

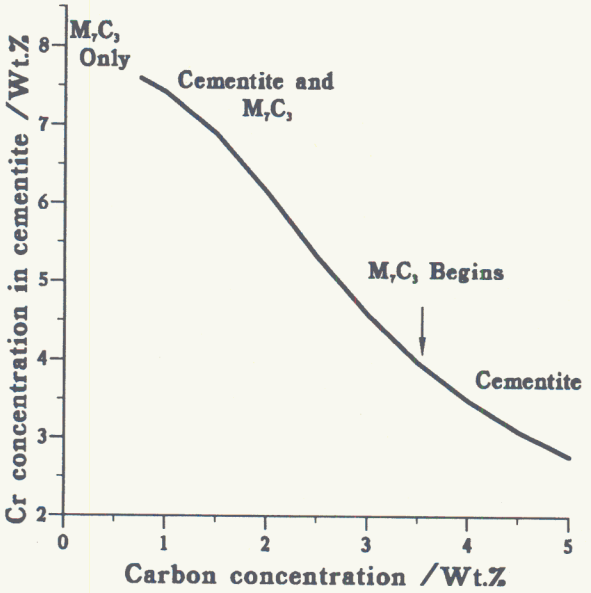

15 Chromium concentration in cementite as function of bulk carbon concentration calculated using Mtdata: overall iron/chromium ratio is kept constant as carbon content is increased

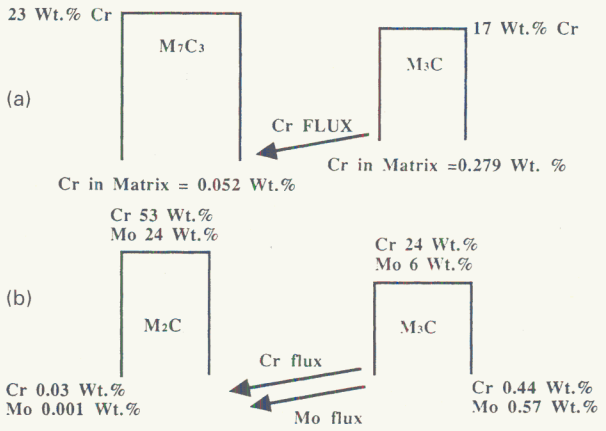

16 Schematic illustration of cementite particle next to *a* M_7C_3 particle and *b* M_2C particle showing calculated equilibrium concentrations in particles and matrix using Mtdata

M_7C_3 carbide typically contained 51%Cr. This could imply a flux of chromium from the cementite to the M_7C_3 when the latter begins to precipitate, if the concentration in ferrite which is in equilibrium with M_7C_3 is smaller than in ferrite in equilibrium with cementite.

The problem cannot be investigated using equilibrium thermodynamics for 2·25Cr–1Mo steel at 565°C because cementite is unstable in a mixture of cementite and M_7C_3. Thus, the carbon concentration assumed for the calculation was increased until the cementite became thermodynamically stable again and coexisted with the M_7C_3 and ferrite. The iron/chromium ratio in the alloy as a whole was kept constant. Figure 15 shows the calculated equilibrium chromium level in cementite as a function of the bulk carbon concentration. It can be seen that for high carbon concentrations only cementite is the stable carbide, and for low carbon concentrations M_7C_3 is stable; for intermediate compositions M_7C_3 and cementite coexist. The lowest carbon concentration at which M_7C_3 and cementite were in equilibrium with ferrite, 0·75%, was chosen to perform further calculations. The cementite–ferrite and M_7C_3–ferrite equilibria were then investigated separately at this overall concentration (Fig. 16*a*). The chromium level in the ferrite matrix surrounding a cementite particle is higher than that surrounding an M_7C_3 particle, a flux of chromium is stimulated from the cementite to the M_7C_3, explaining the drop in chromium level in a cementite particle in the vicinity of an M_7C_3 particle.

COEXISTENCE OF M_2C WITH CEMENTITE

A similar calculation was performed to that described in the previous section to study the coexistence of M_2C and cementite. Once again, in order to allow Mtdata to be used for the coexistence of M_2C and cementite in ferrite, the carbon concentration in the bulk alloy was increased, keeping the iron/chromium ratio constant. Below 0·5%C only M_2C was stable, but further increasing the carbon concentration allowed M_2C and cementite to coexist. As the carbon concentration increased, the volume fraction of cementite was predicted to increase at the expense of the M_2C. The results of the calculation for an overall concentration of 0·5%C are shown in Fig. 16*b*. It can be seen that the increase in the matrix concentration of chromium and molybdenum around a cementite particle would result in a flux of both to the M_2C. This is consistent with the experimentally observed fact that once there is extensive M_2C precipitation within the bainitic plates, the cementite between the plates begins to be depleted in both chromium and molybdenum.

MEASURED DIFFUSION COEFFICIENTS

The enrichment kinetics of cementite particles were studied for various times at three different temperatures in order that the diffusion coefficient and the activation energy could be calculated for the diffusion of chromium in ferrite. The diffusion coefficient of chromium in ferrite D_α can approximately be determined using the analytical equation[3]

$$t_c = \frac{\pi x_\theta^2 (\bar{c} - c^\theta)^2}{16 D_\alpha (c^{\alpha\theta} - \bar{c})^2} \quad \ldots\ldots\ldots\ldots\ldots\ldots (2)$$

where t_c is the time required for the carbide to reach a concentration c^θ, x_θ is the thickness of the carbide plate, D_α is the diffusion coefficient for the substitutional alloying element in ferrite (assumed to also represent the diffusion in the carbide), $c^{\alpha\theta}$ is the concentration of the substitutional solute element of interest, and $\bar{c}$ is the corresponding bulk concentration in the alloy. The most accurate way of performing this calculation is to use all the experimental data gathered and evaluate the quantity

$$\frac{\pi x_\theta^2 (\bar{c} - c^\theta)^2}{16 (c^{\alpha\theta} - \bar{c})^2} \quad \ldots\ldots\ldots\ldots\ldots\ldots (3)$$

for each invididual particle analysed. The tempering times and temperatures used in this analysis only included those specimens in which enrichment of the cementite was taking place rather than the dissolution due to the precipitation of alloy carbides. This therefore included tempering times up to 64 h at 565°C and all the specimens tempered at 510°C, and exlcuded the 25 h specimen tempered at 620°C. The value of $c^{\alpha\theta}$ varies with temperature. The values used in the calculations were determined using Mtdata, allowing only the cementite and ferrite phases to exist (Table 2).

The equilibrium values (Table 2) also take into account the carbon content of the cementite, which the EDX data do not. The EDX measurements were therefore scaled to allow for 6·67%C to be contained in the cementite (the stoichiometric carbon content for M_3C). The regression coefficient was calculated, and therefore the diffusion constant, at each of the three tempering temperatures. Calculated values of diffusion coefficient D_α were $3{\cdot}5 \pm 0{\cdot}2 \times 10^{-19}$, $2{\cdot}5 \pm 0{\cdot}1 \times 10^{-18}$, and $2{\cdot}7 \pm 0{\cdot}3 \times 10^{-17}$ m^2 s^{-1} at temperatures of 510, 565, and 620°C

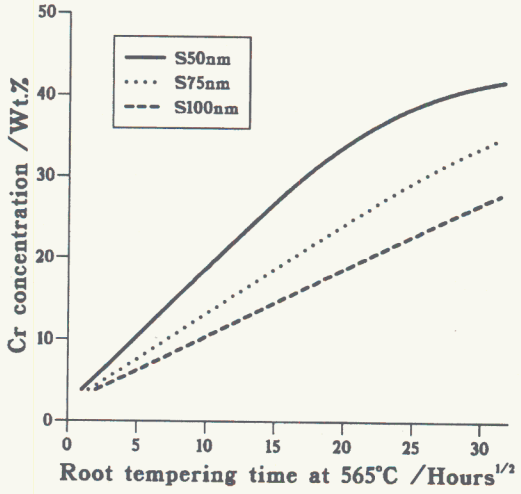

17 Dependence of enrichment of cementite on particle size calculated at 565°C using finite difference model

respectively. The correlation coefficient for these three data points was found to be 0·99.

The calculated values of the diffusion coefficients at the three temperatures were then used to calculate the activation energy for the diffusion of chromium in ferrite using the Arrhenius relationship

$$D = D_0 \exp\left(-\frac{Q}{RT}\right) \quad \ldots\ldots\ldots\ldots\ldots\ldots (4)$$

where Q is the activation energy, R is the universal gas constant, T is the temperature in kelvin and D_0 is the pre-exponential factor. The value for the activation energy of diffusion Q, was calculated as $230\,000 \pm 10\,000$ J mol^{-1}, and the pre-exponential factor was found to be $7{\cdot}0 \pm 0{\cdot}3 \times 10^{-4}$ m^2 s^{-1} (where the errors represent one standard deviation from the mean). These values are in good agreement with those of Fridberg *et al.*[11] for the interdiffusion of chromium in ferrite (an activation energy of 240 000 J mol^{-1}, and a pre-exponential factor of $1{\cdot}5 \times 10^{-4}$ m^2 s^{-1}).

Finally, the experimental results have highlighted the dependence of enrichment on particle size, smaller particles enriching more quickly than larger ones. Figure 17 shows the results of a calculation using the finite difference model of the enrichment rate at 565°C for three different particle sizes: 50, 75, and 100 nm. The model predicts a difference of ~20%Cr between the 50 and 100 nm particles after tempering for 100 h which is consistent with the measured variation of composition with size, and illustrates the importance of making the two measurements simultaneously. This is in contrast to previous work[4] on larger, pearlitic cementite in 0·5Cr–0·5Mo–0·25V steels, in which little dependence of composition on particle size was found.

Conclusions

Experimental studies of cementite composition changes in a bainitic microstructure have been made and compared against a theoretical model for the cementite enrichment process. A strong dependence of enrichment on particle size has been observed, the smaller particles enriching more quickly than the larger ones. Both of these observations are consistent with the predictions of the computer model. Differences in precipitation behaviour between bainitic and martensitic regions of the microstructure have been established. This has important consequences for remanent life assessment in that a simple measurement of cementite composition is not sufficient; the size and position in the microstructure must be simultaneously determined. No significant dependence of the composition of the chromium rich alloy carbide M_7C_3 on size or tempering time has been found. Indications are that once alloy carbides have precipitated, any further enrichment is too small to be useful in estimating the average temperature experienced by the microstructure.

Acknowledgements

The authors would like to thank Professor C. Humphreys for the provision of laboratory facilities at the University of Cambridge. One of the authors (RCT) also wishes to thank the Science and Engineering Research Council and National Power for funding this work. The contribution of one of the authors (HKDHB) was made under the auspices of the Atomic Arrangement: Design and Control project, which is a collaborative venture between the University of Cambridge and the Japan Research and Development Corporation.

References

1. R. B. CARRUTHERS and M. J. COLLINS: in Proc. Conf. 'Quantitative microanalysis with high spatial resolution', 108; 1981, London, The Metals Society.
2. A. AFROUZ, M. J. COLLINS, and R. PILKINGTON: *Met. Technol.*, 1983, **10**, 461–463.
3. H. K. D. H. BHADESHIA: *Mater. Sci. Technol.*, 1989, **5**, (2), 131–137.
4. X. DU, J. A. WHITEMAN, R. C. THOMSON, and H. K. D. H. BHADESHIA: *Mater. Sci. Eng.*, 1992, **A155**, 197–205.
5. R. C. THOMSON: PhD thesis, Cambridge University, 1992.
6. R. G. BAKER and J. NUTTING: *J. Iron Steel Inst.*, 1959, **192**, 257–268.
7. R. SMITH and J. NUTTING: *J. Iron Steel Inst.*, 1957, **187**, 314–329.
8. R. C. THOMSON and H. K. D. H. BHADESHIA: *Mater. Sci. Technol.*, this issue, 205–208.
9. H. K. D. H. BHADESHIA: *Met. Sci.*, 1982, **16**, 159–165.
10. H. K. D. H. BHADESHIA: 'Bainite in steels'; 1992, London, The Institute of Materials.
11. J. FRIDBERG, L.-E. TORNDAHL, and M. HILLERT: *Jernkontorets Ann.*, 1969, **153**, 263–276.
12. S. M. HODSON: Metallurgical and Thermochemical Databank, National Physical Laboratory, Teddington, 1989.
13. J. M. TITCHMARSH: in Proc. 9th Int. Congress on 'Electron microscopy', (ed. J. M. Sturgess), Vol. 1, 618–619; 1978, Toronto, ON, Microscopical Society of Canada.
14. Y. A. BAGARYATSKI: *Dokl. Akad. Nauk. SSSR*, 1950, **73**, 1161.
15. J. M. RACE and H. K. D. H. BHADESHIA: *Mater. Sci. Technol.*, 1992, **8**, (10), 875–882.
16. J. PILLING and N. RIDLEY: *Metall. Trans.*, 1982, **13A**, 557–563.